

Oil Spill Segmentation from SAR Images Using Deep Neural Networks

Alaa Akram Huby¹

¹Collage Information technology
University of Babylon, Babylon, Iraq
alaaa.net.msc@student.uobabylon.edu.iq

Raaid Alubady¹

¹College of Information Technology,
University of Babylon, Iraq
alubadyraaid@itmet.uobabylon.edu.iq

Rafid Sagban^{1,2}

¹Technical Engineering College, Al-
Ayen University, Thi- Qar, Iraq

²College of Information Technology,
University of Babylon, Iraq
rsagban@alaven.edu.iq

Abstract— Large tankers, ships, and pipeline cracks that spew oil onto sea surfaces wreak havoc on the maritime environment. Target scenarios, such as sea and land surfaces, ships, oil spills, and lookalikes, are roughly represented by synthetic aperture radar (SAR) photographs. To assist in leak cleanups and safeguard the environment, oil spills from SAR pictures must be identified and segmented. This research introduces a deep-learning system that uses the U-Net semantic segmentation technique to detect oil spills. With the use of a Densnet201 model that was previously trained on the Imagnet dataset, the encoder portion of Unet was substituted. The Decoder component, in contrast, uses a U-Net framework. Five groups of the dataset are classified using 256256 spatial dimensions and their corresponding annotations. The U-net with the DenseNet201 backbone presented slightly better results (96% accuracy, 79% precision, 80% recall, 80% F-score, and 69% IoU). Moreover, The results of this study are very promising and provide a comparable improved IoU compared to related works.

Keywords—Oil Spill Detection, Artificial Intelligence, Deep Learning, SAR image, Unet Segmentation.

I. INTRODUCTION

An oil spill appears when a liquid petroleum hydrocarbon spills into the environment due to human activities. Oil spills in the maritime environment are more destructive and hazardous than those on flat ground, which is a part of the world's largest issue. They may quickly distribute over hundreds of kilometers, forming a thin oil crust that can blanket coastlines [1]. Therefore, the problem's early detection is necessary in order to avoid serious problems [2]. Improve oil spill detection monitoring systems, observations have been taken around the world using various types of techniques, one of them is Deep Learning (DL).

DL is a subfield of Machine Learning (ML) that can yield exceptional performance. These approaches are more suited for handling massive volumes of data than typical ML techniques. Furthermore, it can automatically learn feature representations from raw data and then produce findings. Moreover, it is reliable and practical [3].

In the last years man yresearchers have developed DL models for Classification [4] and Segmentation [5] and other tasks. On the other side, despite several studies interested in the oil spill issues (see [6] [7] [8] [9] [10]). However, some of them trained the model on a small dataset and other studies fixed the backbone type and the two point effect on the enhancement of accuracy. Hopefully, this work enhances the prediction result by deploying DenseNet201 with Unet and improves the IoU metric because it prefers this metric in the segmentation model. In addition, suggest various preprocessing datasets. Over and above that answer the

questions. How do preprocess the SAR dataset to reduce training of run time? What is the best pre-trained model to deploy with the SAR dataset? Is Unet the better segmentation model? Why? According to that, the present research has three contributions:

- Implement pre-processing steps various from related work in the area
- Compare state-of-the-art deep learning models for this task, and
- Develop a model using SAR images to identify more susceptible regions, 1112 images from 2015 to 2017.

The remainder of this paper is organized as follows. Section 2 provides a background about the Unet, Desnet201 and the related. in Section 3. The explain propose model. After that evaluate propose model in Section 4. results are discussed in Section 5. Finally, the conclusion and summary are presented in Section 6.

II. BACKGROUND AND RELATED WORK

This section will focus on the famous model deployed to detect objects. According to DL classification [11]. Convolutional Neural Networks (CNN) consider the famous model in supervised groups.

A. Dense Convolutional Network (DenseNet201)

There is Vanilla CNNs are usually applied as the backbone which handles encoding and downsampling on their own, including VGG, ResNet, EfficientNet, etc., To create the final Unet, these networks are extracted and their replicas are constructed to execute decoding and upsampling [11-12].

A backbone network is typically employed to extract fundamental features for object detection, and it is typically originally created for image classification and pre-trained on the ImageNet dataset [13]. The Dense Convolutional Network is the main topic of the current study (DenseNet201).

Each layer is immediately connected to the others in a feed-forward manner using the architecture known as DenseNet201. The network has so learned in-depth feature representations for a range of image kinds [14]. It is utilized with semanteic segmentation, as previously described.

B. U-Net Semantic Segmentation Technique

a crucial element in many systems for visual comprehension. Numerous applications, such as medical image, all heavily rely on segmentation [15]. is employed to comprehend spatial texture, geometric shape, as well as color

and gray connection aspects. Additionally, segmented semantic objects can be obtained, and related feature extraction is possible. The goal of image segmentation is to identify the target and extract the characteristics of interest regions [16].

According to [17], there are several models for segmentation:

- Fully Convolutional Network.
- Mask R-CNN (region-based convolutional neural network).
- Encoder-Decoder-Based Models.
- DeepLab.

Unet, which has an expanding path on the left and a contracted path on the right, is one of the encoder-decoder based models [18]. The contracting path follows the convolutional network architecture conventions. The dimensions of the pixel-wise mask created by semantic segmentation models match those of the input image. Most architectures contain contraction and expansion routes, also referred to as encoder and decoder. The encoder's task is to downscale the spatial image dimensions while extracting pertinent characteristics. In order to compare the output categories to the input classifications accurately and similarly, the decoder recovers the image dimensions. Even though the concept is the same across all models, certain quirks may produce superior outcomes depending on the application [19].

C. Related Works

There are numerous models to detect oil spills we collected them in a survey paper (see Ref. [20], under publication) that describes the classification of modern methods for detecting oil spills in the time period (2018-2021). It also explains the use of machine learning, artificial neural networks, and deep learning approaches to address the problem.. But the closest studies to this work are described in detail below and outlined in Table 1.

Deep Convolutional Neural Networks for semantic segmentation were proposed by Krestenitis et al. [6]. (DCNNs). The authors presented a dataset of SAR images that the European Maritime Safety Agency had collected (EMSA). The Model's foundation was fixed, and the best outcomes were obtained when DeepLabV3 was used in conjunction with MobileNetv2. They displayed IoU levels of 65.06 percent.

Moura et al[8] .'s comparison of four backbone.

Table 1. A Summary of Related Works

Ref.	Study Area/ Dataset	Type of Image	Model	Backbone
Krestenitis et al. (2019)	European Maritime Safety Agency (EMSA)	SAR	UNet- LinkNet -PSPNet - DeepLabv2 - DeepLabv2 (mnc) - DeepLabv3+	ResNet101 Except DeepLabv3+ used MobileNetV2
Moura et al. (2022)	Brazilian	SAR	Unet – DeepLabv3+ - LinkNet	ResNet-101, ResNet-50, Efficient-net-B0, and Efficient-net-B3

III. PROPOSEL MODEL

After explaining a brief history of the oil spill problem and indicating the model. Now, it is important to show the significance of our work. Figure 1 shows Macro view of the proposed model.

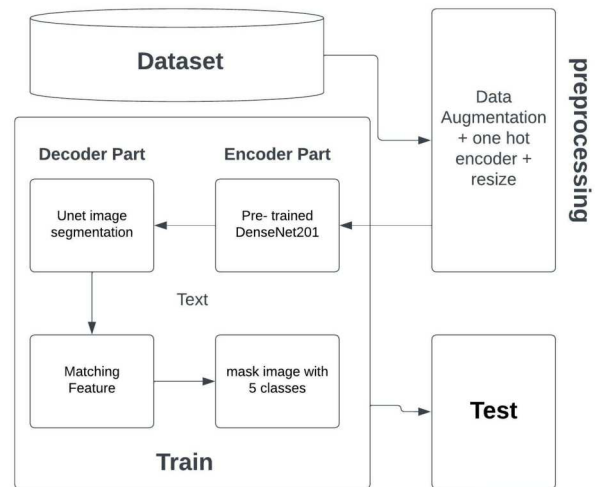


Figure 1. Macro View of the Proposed Model

As shown in the aforementioned figures, Starting with the input of a SAR image dataset, the oil spill location or look-alike detection system is activated. The dataset is split into training data and test data groups. Prior to being sent to the model, all data are pre-processed utilizing resize and enhanced on data. In this paper, a deep learning system for detecting oil spills is introduced. The pre-train model (transform learning) of Densnet201, which was previously trained on the Image dataset, replaces the encoder portion of Unet. In contrast, the Decoder component uses U-Net structure to conduct semantic segmentation. A TF file is the end product of the model creation. By examining the best training loss, training IoU, and test loss, the former model is assessed.

While the micro view of the proposed model can be illustrated in Figure 2.

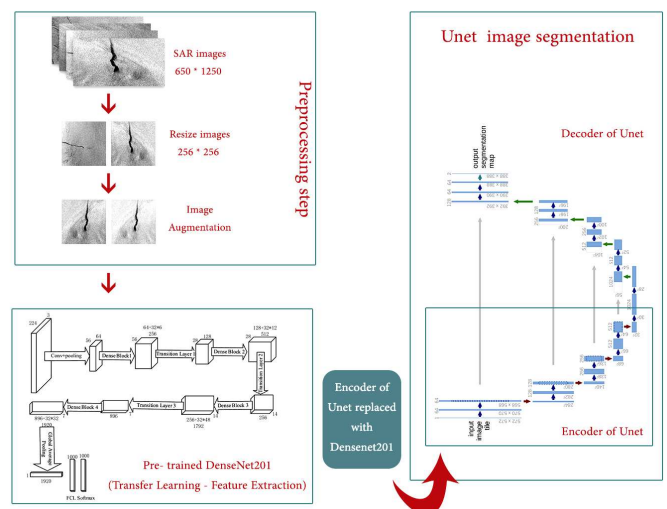


Figure 2. Micro View of the Proposed Model

A. Pre-processing Stage

1) Resize image

The dataset images size 1250 x 750 that size not compatible with the target model size. So, resizing an image is one of the important preprocessing steps. In this model, the images resize to be 256x256.

2) One Hot Encoding

One popular encoding technique entails converting categorical data into a format that can be supplied to DL algorithms to aid in their prediction performance. One Hot Coding is the most well-liked coding method [21]. There are five classes in this study that describe how the original values are represented as one hot encoded vector when there are five distinct targets (See Table 2).

Table 2. One Hot Encoder for Five Classes

Before One Hot Encoding	After One Hot Encoding
0	[1, 0, 0, 0, 0]
1	[0, 1, 0, 0, 0]
2	[0, 0, 1, 0, 0]
3	[0, 0, 0, 1, 0]
4	[0, 0, 0, 0, 1]

3) Data Augmentation

The ImageDataGenerator class from the Keras package, which greatly simplifies the use of geometric augmentations, is used in this study's data augmentation [22]. The generator or augmentation used in this study only applies to the dataset train and rotates images randomly to the left or right while also using random saturation, random brightness, and clip by value to maintain the image's [0, 1] range. Following the completion of the preprocessing stage, the model has two stages.

B. Deep Learning Model Stage

The pixel-wise mask produced by semantic segmentation models has the same dimensions as the input image. Contraction and expansion routes, commonly referred to as the encoder and decoder, are found in the majority of architecture. The encoder's job is to downscale the spatial image dimensions while extracting important characteristics. In order to compare the output categories of the input classifications accurately and similarly, the decoder recovers the image dimensions. The architecture was taken into consideration in this study: U-net.

There are several parallels between the U-net and LinkNet. In contrast to the U-net, the LinkNet concatenates the encoder and decoder rather than adding them together. Recently, the field of computer vision has paid a lot of attention to the improved CNN development. Additionally, we contrasted the DenseNet201 encoders, which produced distinctive pairings. The DenseNet201, one of the most well-known CNNs, popularized the concept of residual learning and avoided problems like vanishing gradients. Combining architecture with backbones is a pretty straightforward operation because the backbones serve as the encoder section of the architecture. The segmentation models tensor flow, which are very high-level and make it easy to test and contrast different settings, were used to generate the models.

1) Pre-train DenseNet201

The first part is a feed-forward connection between each layer in a DenseNet201 design. DenseNet201 has the advantages of being light on the gradient problem, allowing feature reuse, feature deployment, and its functionality minimizes the amount of parameters. The input image size for the network is 224x224. It is content four Dense block. At each Dense block we have a repetition of:

- 1x1 conv with k filters
- 3x3 conv with k filters blocks.

Each "conv" layer corresponds to the order BN-ReLU-Conv as written. Each block's input, which takes the form of a matrix corresponding to the picture pixel, will then be passed to the batch normalization stage, Three transition layers, each with a "conv" and average pool, are also present [23].

2) Unet Segmentation

Unet is the second component. It consists of an expansive path (right side), which is represented by DenseNet201, and a contracting path (left side) (right side). Each 64-component feature vector is mapped to the chosen number of classes in the final layer using a 1x1 convolution [19].

IV. DATASET AND PERFORMANCE MODEL

A. Dataset

The Synthetic Apertures Dataset (SAR) was used in this investigation [24]. 1112 photos total, divided into five categories (sea, oil spill, look-alike, hip, and land). Figure 3 displays a sample SAR dataset.

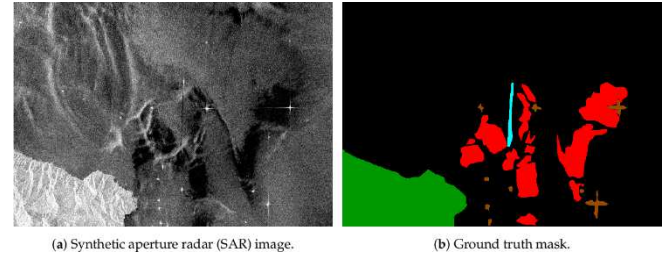


Figure 3. Original SAR Image with Mask

Red, Green, and Blue (RGB) color images are used exclusively in this study's images. In the pre-processing stage, the 1250 x 650 original image is downsized to a resolution of 256x256. Resizing is then done to change the amount of processing being done using the DenseNet201 model. With a suitable representation of the model's format, this study used the preprocess input function of DenseNet201-ResNet101-efficientnetb3). 90% of the dataset is used for training, while 10% is used for testing, as shown in Tabel 3 below.

Tabel 3. Dataset Divided

Set	Number of Images	Percentage(%)
Train	1002	90%
Test	110	10%

B. Performance Evaluation Metrics

Numerous evaluation measures are provided to measure the efficiency of various segmentation models. An image segmentation model produces a prediction after training. It is necessary in order to evaluate the model in order to determine its performance. The following are the evaluation measures

that are widely employed by the literature see the Ref. [17] for image segmentation tasks.

➤ *Intersection over Union (IoU)*

IoU calculates the performance using the intersection and union between the Prediction and Ground Truth values. IoU falls between 0-1 (0-100%), where 0 signifies no overlap and 1 signifies perfectly overlapping segmentation. The following is the equation for defining IoU.

$$\text{IoU} = \text{Area of Overlap} / \text{Area of Union} \dots\dots\dots (1)$$

➤ *Pixel Accuracy*

Pixel accuracy takes the ratio of correctly classified pixels with respect to total pixels. The following is the equation for defining pixel accuracy.

$$\text{Accuracy} = (\text{TP} + \text{TN}) / (\text{TP} + \text{TN} + \text{FP} + \text{FN}) \dots\dots\dots (2)$$

➤ *Precision*

Precision is the ratio between True Positives and all the Positives. The following is the equation for defining precision.

$$\text{Precision} = \text{TP} / (\text{TP} + \text{FP}) \dots\dots\dots (3)$$

➤ *Recall*

Recall defines as a measure that correctly identifies True Positives. The following is the equation for defining recall.

$$\text{Recall} = \text{TP} / (\text{TP} + \text{FN}) \dots\dots\dots (4)$$

➤ *F1 Score*

The F1 score is the weighted average of Precision and Recall. When the dataset's class distribution was uneven, it was helpful. Here is the formula for calculating the F1-Score.

$$F1 = 2 * ((\text{Precision} * \text{Recall}) / (\text{Precision} + \text{Recall})) \dots\dots (5)$$

V. RESULT AND DISCUSSION

In this study, tests make use of a 256x256x3 picture. Red, Green, and Blue are the three colors that make up the number "3". This approach transforms learning using CNN models, specifically DenseNet201. Five classes and the anticipated mask are detected using the Unet model. To examine the IoU and accuracy performances, we adjusted the parameter epoch 50. At this training stage, we save a model with a lower training loss value than the prior epoch.

This study used batch sizes of 12 and Adam optimizers. The validation outcomes for training data using DenseNet201 as the foundation of the Unet model are shown in Table 4 and Figure 5 below.

Tabel 4. Validation Proposal Model

Model	Unet	Unet	Unet	Linknet	Linknet	Linknet
Backbone	DenseNet 201	Resnet101	Efficientnetb3	DenseNet 201	Efficientnetb3	Resnet101
No. of Parameters	26379157	51606046	17868413	22549973	13761565	47828318
Accuracy	0.9653	0.9644	0.9638	0.9658	0.9657	0.9575
Precision	0.7961	0.8002	0.7872	0.6823	0.791	0.6414
Recall	0.8001	0.7401	0.7647	0.6377	0.7698	0.6924
F-score	0.8032	0.7657	0.7822	0.6547	0.7885	0.6728

IoU	0.6997	0.6654	0.6757	0.5853	0.6845	0.5868
Epoch	50	50	50	50	50	50
Batch size	12	12	12	12	12	12
Loss	0.2039	0.248	0.257	0.3397	0.233	0.3632
Execution time of Training	0:15:57.720 sec	0:15:24.730 sec	0:18:59.184 sec	0:14:56.953 sec	0:20:39.887 sec	0:15:25.870 sec
Execution Time of Testing	1s 133 ms/step	1s 138 ms/step	1s 127 ms/step	1s 129 ms/step	1s 130 ms/step	1s 137 ms/step

According to the above table, we note that the best results were achieved through implement Densenet 201 with Unet.

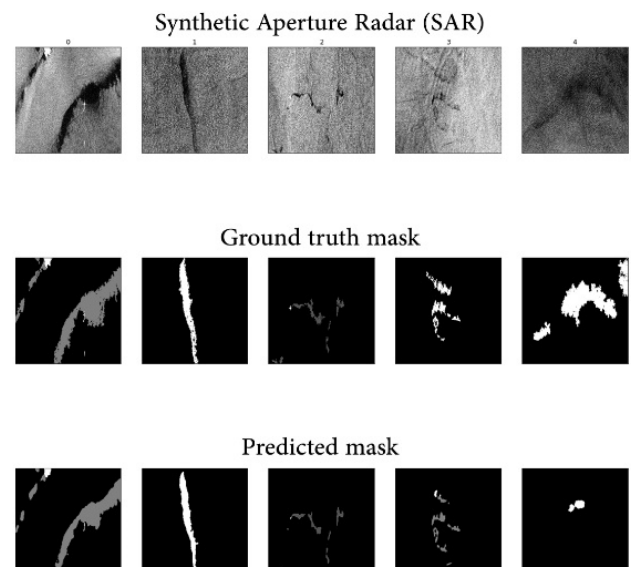


Figure 5. Five examples of the original 256x256 image with the ground truth and the predictions from the best (U-net architecture with DenseNet201).

After validation step the proposed model result compare with previous study in same area to evaluate the model as show in Table 5.

Tabel 5. Evaluation proposal model

	Proposed Model	Krestenitis et al. (2019)	Moura et al. (2022)
Model	Unet	DeepLapV3+	Unet
Backbone	DenseNet201	MobileNetV2	efficientnetb3
Number of Parameters	26379157	51606046	12565417
Accuracy	0.9653	--	0.98
Precision	0.7961	--	0.75

Recall	0.8001	--	0.78
F-Score	0.8032	--	0.76
IOU	0.6997	65.06	0.62
Epoch	50	50	37
Batch Size	12	12	12

As show in table above the proposed model record the highest IoU When compared with related work.

VI. CONCLUSION

This research focuses on improving the IoU of oil spill detection systems or not. Previous research using the Resnet, MobileNet various version and model resulted in less than 65% IoU. In this study at first pre-process dataset in three stage (resize image, Data augmentation and apply one hot encoder on there mask) after that used the DenseNet201 model as encoder part and Unet represented the decoder part. The result showed that the detection system produces an IoU value of 69.%. In future work, we will focus on oil spill detection by training the model with real-time oil spill spots and deploying the model in multi-node instate of single to reduce execution time.

References

- [1] H. Jafarzadeh, M. Mahdianpari, S. Homayouni, F. Mohammadimanesh, and M. Daboor, "Oil spill detection from Synthetic Aperture Radar Earth observations: a meta-analysis and comprehensive review," *GIScience Remote Sens.*, vol. 58, no. 7, pp. 1022–1051, 2021, doi: 10.1080/15481603.2021.1952542.
- [2] R. Jafari, S. Razvarz, A. Gegov, and B. Vatchova, "Deep Learning for Pipeline Damage Detection: An Overview of the Concepts and a Survey of the State-of-the-Art," *2020 IEEE 10th Int. Conf. Intell. Syst. IS 2020 - Proc.*, pp. 178–182, 2020, doi: 10.1109/IS48319.2020.9200137.
- [3] H. Liu and B. Lang, "Machine learning and deep learning methods for intrusion detection systems: A survey," *Appl. Sci.*, vol. 9, no. 20, 2019, doi: 10.3390/app9204396.
- [4] Y. Li *et al.*, "Detection of Oil Spill Through Fully Convolutional Network," *Commun. Comput. Inf. Sci.*, vol. 848, no. June, pp. 353–362, 2018, doi: 10.1007/978-981-13-0893-2_38.
- [5] H. Guo, G. Wei, and J. An, "Dark spot detection in SAR images of oil spill using segnet," *Appl. Sci.*, vol. 8, no. 12, 2018, doi: 10.3390/app8122670.
- [6] M. Krestenitis, G. Orfanidis, K. Ioannidis, K. Avgerinakis, S. Vrochidis, and I. Kompatsiaris, "Oil spill identification from satellite images using deep neural networks," *Remote Sens.*, vol. 11, no. 15, pp. 1–22, 2019, doi: 10.3390/rs11151762.
- [7] M. Shaban *et al.*, "A deep-learning framework for the detection of oil spills from SAR data," *Sensors*, vol. 21, no. 7, 2021, doi: 10.3390/s21072351.
- [8] N. V. A. de Moura, O. L. F. de Carvalho, R. A. T. Gomes, R. F. Guimarães, and O. A. de Carvalho Júnior, "Deep-water oil-spill monitoring and recurrence analysis in the Brazilian territory using Sentinel-1 time series and deep learning," *Int. J. Appl. Earth Obs. Geoinf.*, vol. 107, p. 102695, Mar. 2022, doi: 10.1016/J.JAG.2022.102695.
- [9] X. Yaohua and M. Xudong, "A SAR oil spill image recognition method based on densenet convolutional neural network," *Proc. - 2019 Int. Conf. Robot. Intell. Syst. ICRIS 2019*, pp. 78–81, 2019, doi: 10.1109/ICRIS.2019.00028.
- [10] K. Zeng and Y. Wang, "A deep convolutional neural network for oil spill detection from spaceborne SAR images," *Remote Sens.*, vol. 12, no. 6, 2020, doi: 10.3390/rs12061015.
- [11] S. Dargan, M. Kumar, M. R. Ayyagari, and G. Kumar, "A Survey of Deep Learning and Its Applications: A New Paradigm to Machine Learning," *Arch. Comput. Methods Eng.*, vol. 27, no. 4, pp. 1071–1092, Sep. 2020, doi: 10.1007/s11831-019-09344-w.
- [12] "What is the use of BackBone in UNET model ? | Data Science and Machine Learning | Kaggle." <https://www.kaggle.com/general/205141> (accessed Sep. 20, 2022).
- [13] T. Liang *et al.*, "CBNetV2: A Composite Backbone Network Architecture for Object Detection," *AAAI 2020 - 34th AAAI Conference on Artificial Intelligence*, pp. 11653–11660, 2021, [Online]. Available: <https://arxiv.org/abs/2107.00420v6>.
- [14] F. Dharma Adhinata, D. Putra Rakhmadani, M. Wibowo, and A. Jayadi, "A Deep Learning Using DenseNet201," vol. 9, no. 1, pp. 115–121, 2021.
- [15] S. Minaee, Y. Boykov, F. Porikli, A. Plaza, N. Kehtarnavaz, and D. Terzopoulos, "Image Segmentation Using Deep Learning: A Survey," *IEEE Transactions on Pattern Analysis and Machine Intelligence*, vol. 44, no. 7, pp. 3523–3542, 2022, doi: 10.1109/TPAMI.2021.3059968.
- [16] E. K. Wang, C. M. Chen, M. M. Hassan, and A. Almogren, "A deep learning based medical image segmentation technique in Internet-of-Medical-Things domain," *Futur. Gener. Comput. Syst.*, vol. 108, pp. 135–144, 2020, doi: 10.1016/j.future.2020.02.054.
- [17] Sanskruti Patel, "Deep Learning Models for Image Segmentation," *International Conference on Computing for Sustainable Global Development*, pp. 149–154, 2021, doi: 10.1109/INDIACom51348.2021.00027.
- [18] I. A. Kazerouni, G. Dooley, and D. Toal, "Ghost-UNet: An Asymmetric Encoder-Decoder Architecture for Semantic Segmentation from Scratch," *IEEE Access*, vol. 9, pp. 97457–97465, 2021, doi: 10.1109/ACCESS.2021.3094925.
- [19] H. Su, F. Xing, X. Kong, Y. Xie, S. Zhang, and L. Yang, "Robust cell detection and segmentation in histopathological images using sparse reconstruction and stacked denoising autoencoders," *Advances in Computer Vision and Pattern Recognition*, no. 9783319429984, pp. 257–278, 2017, doi: 10.1007/978-3-319-42999-1_15.
- [20] Alaa Akram Hubby, Raaid Alubady, Rafid Sagban "Oil Spill Detection based on Machine Learning and Deep Learning: A Review," *under publication*, pp. 1-6, 2022.
- [21] Kedar Potdar, Taher S. Pardawala, and Chinmay D. Pai, "A Comparative Study of Categorical Variable Encoding Techniques for Neural Network Classifiers," *Int. J. Comput. Appl.*, vol. 175, no. 4, p. 375, 2017.
- [22] C. Shorten and T. M. Khoshgoftaar, "A survey on Image Data Augmentation for Deep Learning," *Journal of Big Data*, vol. 6, no. 1, 2019, doi: 10.1186/s40537-019-0197-0.
- [23] B. Hogenmüller, "Cano und Terenz Spuren des terenzischen Eunuchus in De locis theologicis," *Rheinisches Museum für Philologie*, vol. 154, no. 3–4, pp. 413–416, 2011.
- [24] "Oil Spill Detection Dataset · MKLab." <https://mklab.iti.gr/results/oil-spill-detection-dataset/> (accessed Sep. 20, 2022).
- [25] S. A. G. Ali, H. R. D. AL-Fayyadh, S. H. Mohammed, and S. R. Ahmed, "A Descriptive Statistical Analysis of Overweight and Obesity Using Big Data," 2022 International Congress on Human-Computer Interaction, Optimization and Robotic Applications (HORA), Jun. 2022, doi: 10.1109/hora55278.2022.9800098.
- [26] S. R. Ahmed, E. Sonuc, M. R. Ahmed, and A. D. Duru, "Analysis Survey on Deepfake detection and Recognition with Convolutional Neural Networks," 2022 International Congress on Human-Computer Interaction, Optimization and Robotic Applications (HORA), Jun. 2022, doi:

- [27] H. A. Jasim, S. R. Ahmed, A. A. Ibrahim, and A. D. Duru, "Classify Bird Species Audio by Augment Convolutional Neural Network," 2022 International Congress on Human-Computer Interaction, Optimization and Robotic Applications (HORA), Jun. 2022, doi: 10.1109/hora55278.2022.9799968
- [28] I. Shaban, M. A. Farhan, and S. R. Ahmed, "Building a Smart System for Preservation of Government Records in Digital Form," 2022 International Congress on Human-Computer Interaction, Optimization and Robotic Applications (HORA), Jun. 2022, doi: 10.1109/hora55278.2022.9800034
- [29] OlaF. Ahmed, R. H. Thaher, and S. R. Ahmed, "Design and fabrication of UWB microstrip Antenna on different substrates for wireless Communication system," 2022 International Congress on Human-Computer Interaction, Optimization and Robotic Applications (HORA), Jun. 2022, doi: 10.1109/hora55278.2022.9799852
- [30] L. I. Khalaf, S. A. Aswad, S. R. Ahmed, B. Makki, and M. R. Ahmed, "Survey On Recognition Hand Gesture By Using Data Mining Algorithms," 2022 International Congress on Human-Computer Interaction, Optimization and Robotic Applications (HORA), Jun. 2022, doi: 10.1109/hora55278.2022.9800090
- [31] S. R. A. Ahmed and E. Sonuç, "Deepfake detection using rationale-augmented convolutional neural network," Applied Nanoscience, Sep. 2021, doi: 10.1007/s13204-021-02072-3
- [32] Ahmed, S. R. A., UÇAN, O. N., Duru, A. D., & Bayat, O. (2018). Breast cancer detection and image evaluation using augmented deep convolutional neural networks. *Aurum journal of engineering systems and architecture*, 2(2), 121-129.